Electronic supplementary Information (ESI)

For

Ultra-efficient and Stable Heterogeneous Fenton Nanocatalysts for Degrading Organic Dyes via Chelating Effect at Neutral Conditions under Nanoconfinement

Jiayou Lin[a, #], Sheng Chen[a, #], Hongyan Xiao[a], Jiawen Zhang[b], Jianwu Lan[a], Bin Yan[a,b*], Hongbo Zeng[b]

a National Engineering Laboratory for Clean Technology of Leather Manufacture, College of Biomass Science and Engineering, Sichuan University, Chengdu, 610065, China

b. Department of Chemical and Materials Engineering, University of Alberta, Edmonton, Alberta T6G 1H9, Canada

# JYL and SC contributed equally to this work.

**Email: yanbinscu@126.com (B.Y.)*

1. Chemicals. Dopamine hydrochloride (DA), tetraethylorthosilicate (TEOS) (99%), $FeCl_3 \cdot 6H_2O$ were purchased from Sigma Aldrich. $NH_3 \cdot H_2O$ (25%), $NaHCO_3$, Tris(hydroxymethyl)aminomethane, ethanol, methylene blue (MB), Neutral Red (NR), Rhodamine B (RHB), Congo Red (CR), HCl and NaOH were purchased from Chemical Co. Ltd, Chengdu, China. All chemicals were analytical grade and used without further purification. The autoclave was obtained from ShengJinKang Instrument Co. Ltd, Chengdu, China. Deionized water (18.2 MΩ cm) used for all experiments was produced from Experimental Water System (2YUPT-II-IUT).

2. Characterizations. The morphology of samples was studied by a field emission scanning electron microscopy (FE-SEM) (JSM-5900LV, JEOL) operated at 15 kV and transmission electron microscopy (TEM) (Tecnai G2 F20 S-TWIN, FEI) at 200 kV. Fourier-transfer infrared (FTIR) spectra were recorded on a Nicolet 6700 spectrometer. The spectra were recorded over a wavelength range from 400 to 4000 cm^{-1}. The specific surface areas of MPOPs were measured on a Micromeritics Gemini 3.04 nitrogen-adsorption apparatus (Micromeritics Instrument Corporation, America) using the Brunauer-Emmett-Teller (BET) method at a relative pressure ratio ranging from 0 to 1 at 77 K. Powder X-ray diffraction (XRD) measurements were performed using Xcalibur E diffractometer. Magnetic characterization was measured by a superconducting quantum interfere device (SQUID) magnetometry with applied magnetic field ranging from -3 T to 3 T at 300 K. To figure out the catalysis process, p-phthalic acid (PTA) was introduced to form 2-hydroxyterephthalic acid with hydroxyl radicals, which could be determined by Fluorescence spectrophotometer (F7100). Zeta potential measurements were performed on Nano ZSP (ZEN5600, Malvern instruments Co. Ltd)

3. Synthesis of Magnetic Fe_3O_4 nanoparticles. The magnetic nanoparticles were synthesized according to a reported procedure.[1] In brief, $FeCl_3$ solution (0.3 mM, 10 mL) was added into aqueous $NaHCO_3$ solution (0.45 mM, 20

mL). After vigorously stirring for 30 min, an aqueous solution of vitamin C (88 mg, 10 ml) was added dropwise into the above mixture. Then, the resulting mixture was transferred into an autoclave and heated at 150 ^{o}C for 4 h. The black products were collected magnetically followed with washing ethanol and water several times. Finally, the magnetic nanoparticles were dispersed into water and stored at 4 ^{o}C for further use.

4. Synthesis of magnetic nanoparticles impregnated porous PDA organic nanocomposites (MPOPs). Briefly, ethanol (12 mL) and deionized water (40 mL) were mixed with concentrated ammonium solution (0.5 ml, 6 M). After 30 min mixing, Fe_3O_4 nanoparticles (0.2 g) and TEOS (0.5 mL) were added successively into the above mixture. After 24 h reaction, an aqueous solution of DA (0.05 g/mL, 4 mL) was added and the resulting mixture was stirred for another 24 h. The resulting compact Fe_3O_4@PDA/SiO_2 nanocomposites were collected by centrifuging at 8000 rpm for 10 min. To obtain the mesoporous structure, the above product was dispersed in Tris-HCl buffer solution (10 mM, 40 mL) and transferred into an autoclave, which was heated at 140 ^{o}C for another 24 h. Finally, MPOPs were collected by centrifugation followed with washing with deionized water and ethanol for several times. The as-prepared MPOPs were first dispersed in deionized water and the pH of the MPOPs solution was adjusted to 7. The whole mixture was sonicated for 20 min to obtain a homogenous solution. Then, 20 mL of the above solution was dried under vacuum at 100 ^{o}C for 24 hr to determine the exact concentration of the MPOP solution in mg/mL. For the degradation experiment, a certain volume of the solution was taken so that the desired weight of the input MPOPs can be adopted.

5. Degradation experiments of MB. Typically, batch experiments of MB degradation in aqueous solution by using the as-prepared MPOPs were carried out in a shaker at 280 rpm at 25 ^{o}C. In these experiments, MB solutions with desired concentrations (from 40 to 300 ppm) were obtained through the dilution

of stock solution (500 ppm). To study the effect of MB concentration on the degradation performance of MPOPs, H_2O_2 solution (30%, 1 mL) and MPOPs (2 mg) were added into the above mentioned MB solutions (20 mL). After different time intervals, the mixed solutions (2 mL) were collected by using 0.22 μm PES membrane filters and then the remaining MB concentration was determined using a UV-vis spectrophotometer (UV-2700). The degradation efficiency by MPOPs was determined according to the equation below:

$$Removal\ efficiency = \frac{(C_0 - C_t)}{C_0} \times 100\% \quad (1)$$

where C_0 *and* C_t (*ppm*) are the initial concentration and the residual concentration of MB solution at time *t* (min).

The effect of the pH on degradation of MB solution was also investigated. First, the pH of MB solution was adjusted to a desired value using 0.1 M HCl/NaOH solutions with the help of a pH meter (Mettler Toledo Co., Ltd., Shanghai, China). Then H_2O_2 solution (30%, 1 mL) and MPOPs (2 mg) were added into the MB solutions (80 ppm, 20 mL) with certain pH. The degradation efficiency under different pH at different time intervals was obtained by the above experimental protocol.

In order to investigate the degradation mechanism, different reagents (i.e., 2 mg of MPOPs and 1 mL H_2O_2, 2 mg of MPOPs, 2 mg of Fe_3O_4 and 1 mL of H_2O_2, 1 mL of H_2O_2) were added into MB solutions (80 ppm, 20 mL) at neutral pH of 7. The degradation efficiency at different time intervals was obtained using the same protocol as mentioned above.

These data were fitted by using the pseudo-first order kinetic model:

$$-ln(C_t/C_0) = K \times t \quad (2)$$

where C_0 *and* C_t (*ppm*) are initial concentration of MB solution and the residual MB concentration for time t (min), *K* is the constant of pseudo-first order kinetic.

6. Fe-leaching experiments. Typically, MPOPs (2 mg) was added into a mixture of MB solution (20 mL, 80 ppm) and H_2O_2 solution (30 wt%, 1 mL). After reaction, the solution was collected through a 0.22 μm PES membrane filter for ICP measurement to determine the Fe leaching in solution.

7. MPOPs cycling experiments. Typically, MPOPs (2 mg) were added into 20 mL of MB solution (80 ppm, pH 7) containing 1 mL H_2O_2. The mixture was stirred at 25 °C for 60 min, and then collected by centrifugation (8000 rmp, 5 min). The collected MPOPs were regenerated by washing with ethanol instead of DI water. Compared to that regenerated with DI water, we found that it is much easier to collect the used MPOPs by centrifugation via ethanol regeneration, although the activity of MPOPs after washing with DI water is almost the same as that with ethanol. The regenerated MPOPs were reused in the successive degradation experiment. The above procedures were repeated for 4 times. The mass loss of the MPOPs was also determine after the last cycling experiment by collecting the MPOPs by centrifugation followed with drying at vacuum at 100 °C overnight. It turned out that only 6% of the MPOPs have been lost after 4 times cycling.

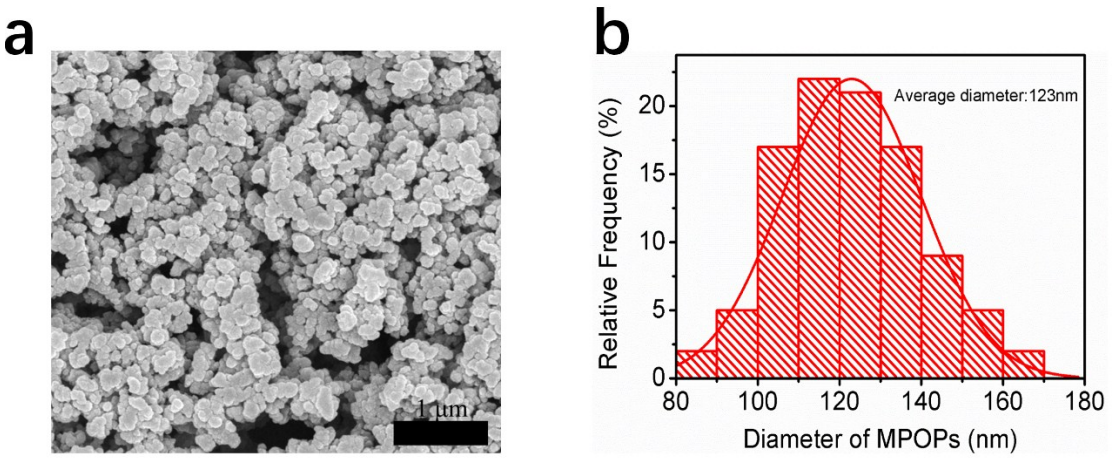

Fig. S1 a) The SEM image and b) the diameter distribution of MPOPs.

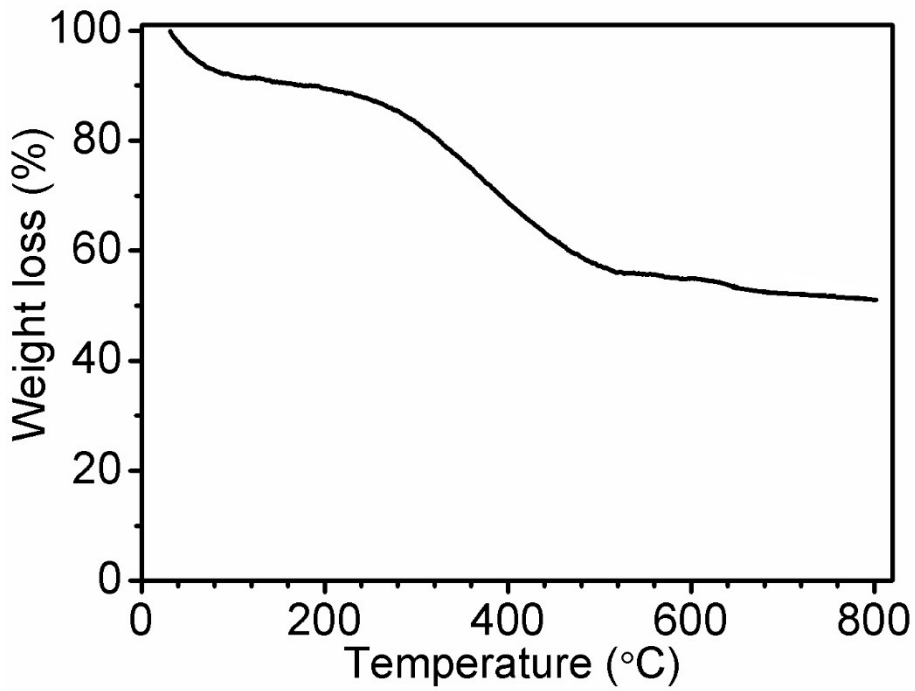

Fig. S2 Thermogravimetric analysis (TGA) plot curve of MPOPs under with nitrogen atmosphere.

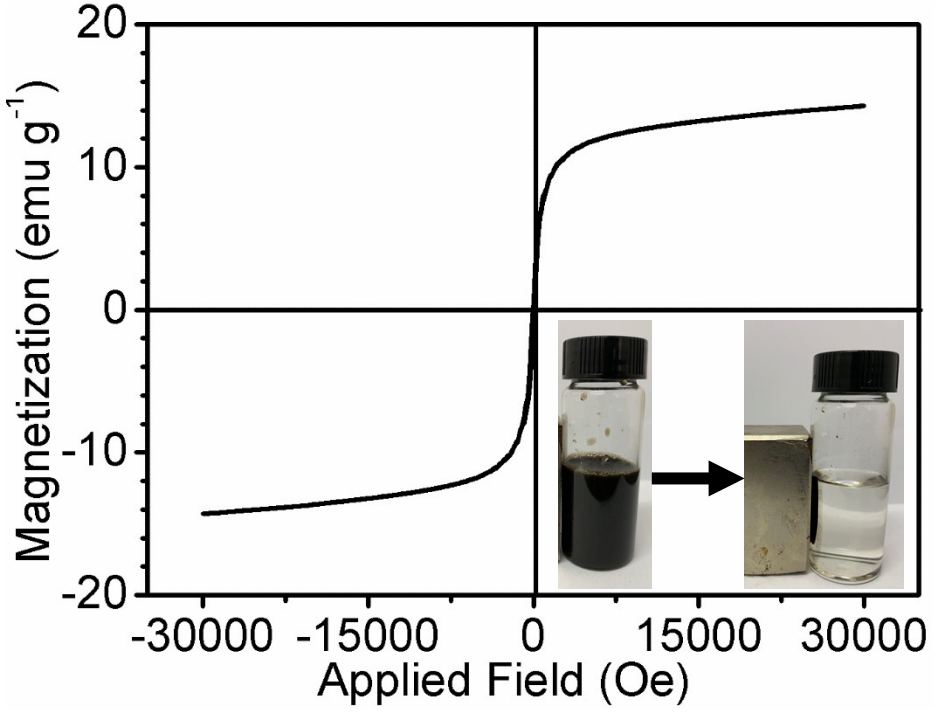

Fig. S3 The hysteresis loop of MPOPs measured at 300 K (the inset shows the dispersion of MPOPs in water and after an external magnetic field is applied). The saturation magnetization value for MPOPs is about 15 emu g^{-1}, which allows fast separation of the dispersed MPOPs from the solution using an external magnetic field.

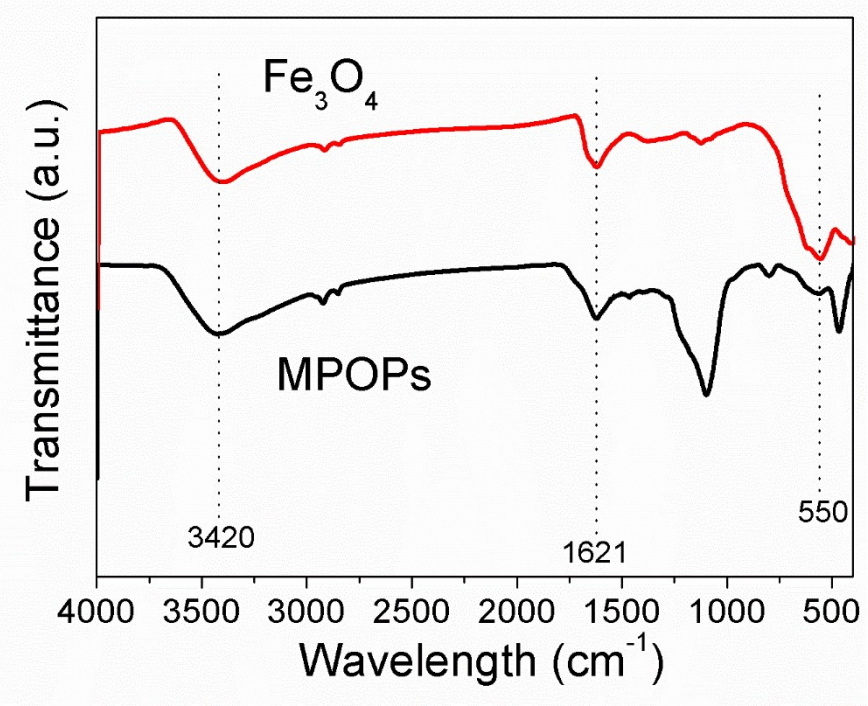

Fig. S4 FT-IR spectra of Fe_3O_4 and MPOPs. The FTIR spectra of MPOPs clearly exhibit characteristic adsorption peaks of both PDA and Fe_3O_4, including the adsorption bands at 3420 cm^{-1}, 1621 cm^{-1}, and 550 cm^{-1} attributed to the stretching vibration of phenolic O–H and N–H, the stretching vibration of aromatic ring and bending vibration of N–H, and the Fe–O vibration of Fe_3O_4, respectively.

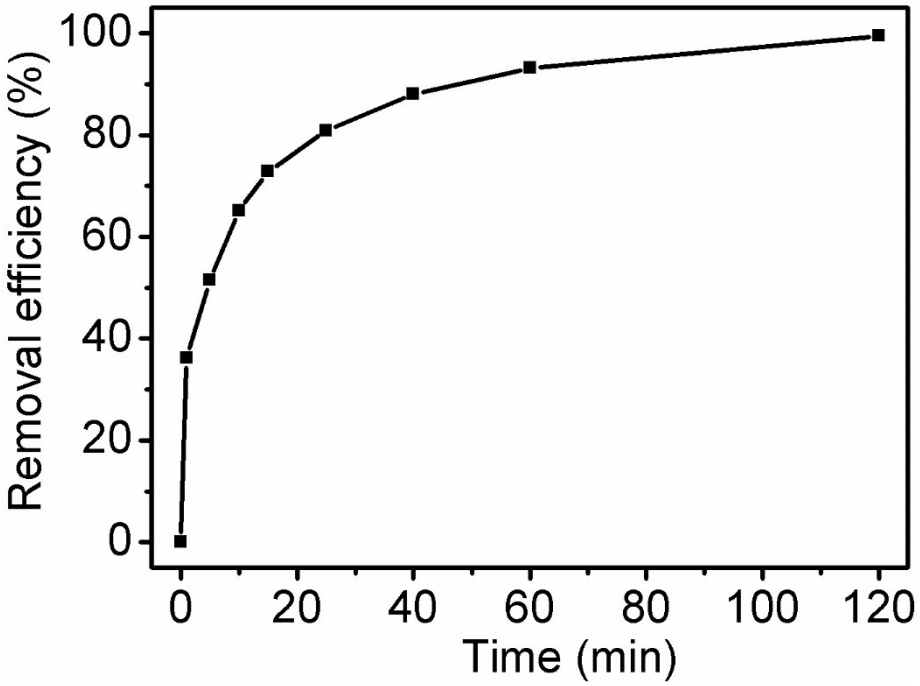

Fig. S5 The degradation experiment of MPOPs to MB at pH 2 with prolonging the reaction time to 2 hr.

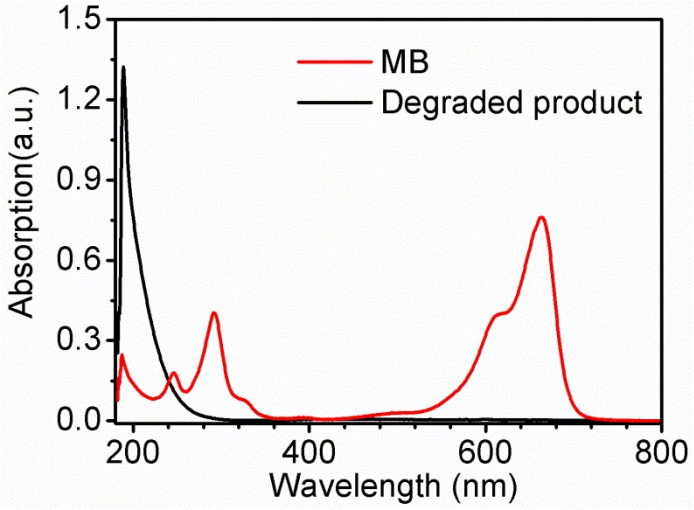

Fig. S6 The UV adsorption spectra of MB and the supernatant from washing from the MPOPs after Fenton reaction.

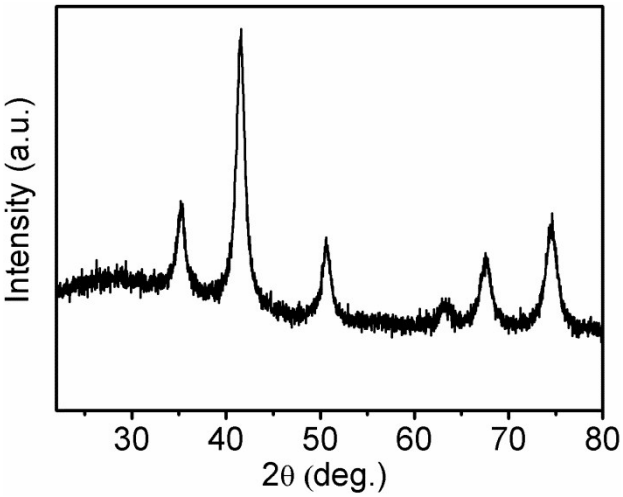

Fig. S7 The XRD of the MPOPs after the Fenton process.

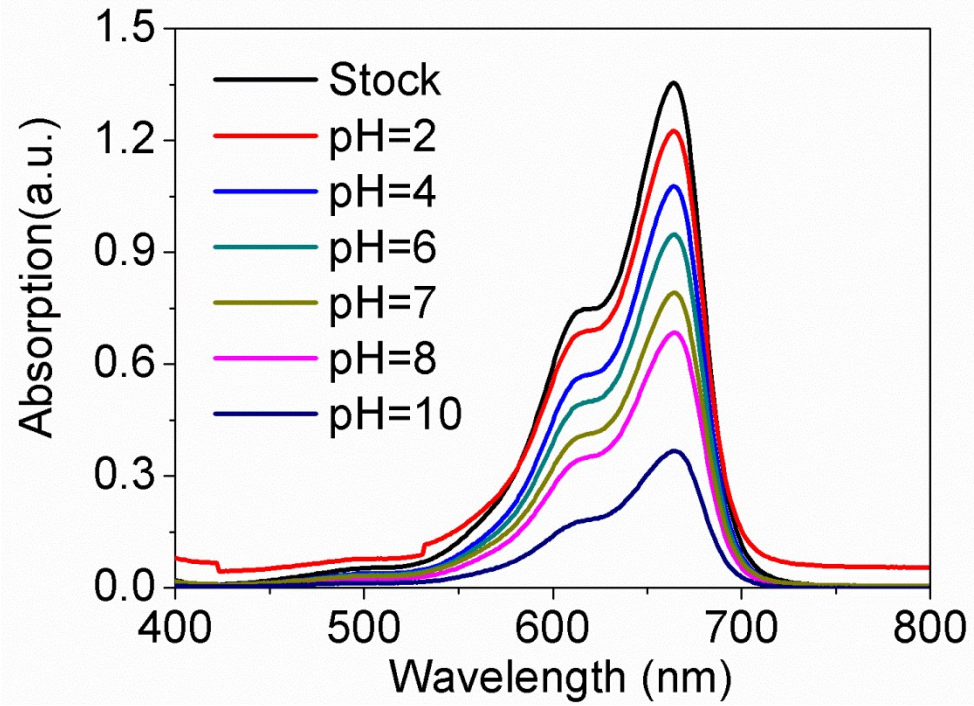

Fig. S8 The adsorption experiments of MPOPs to MB at different pH conditions without H_2O_2.

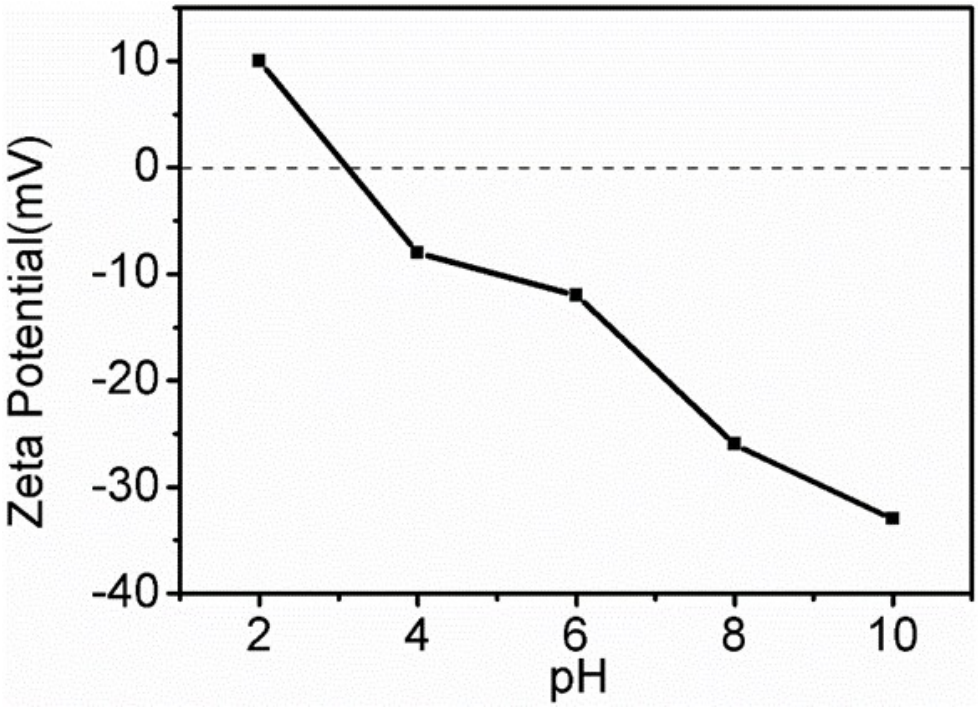

Fig. S9 The zeta potential of MPOPs as a function of pH.

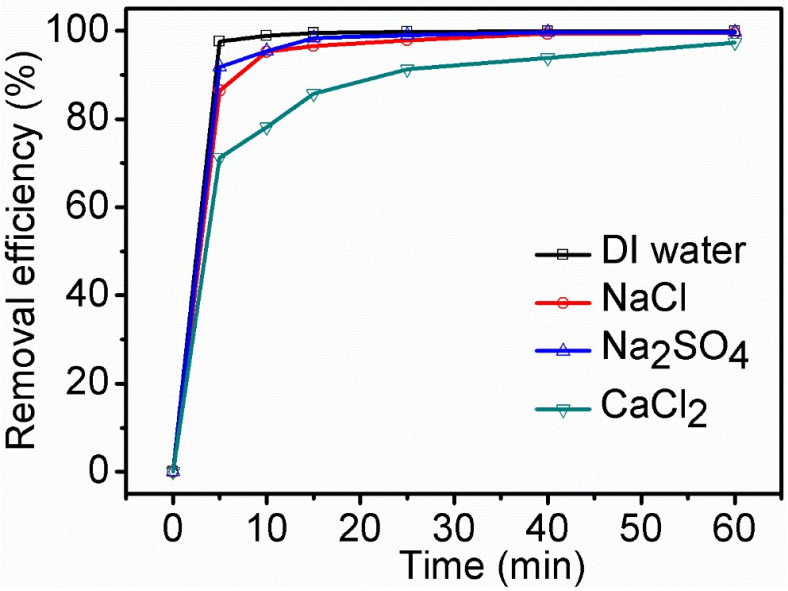

Fig.S10 Effect of co-existing ions, including NaCl, Na_2SO_4 and $CaCl_2$, on removal efficiency of MPOPs to MB (experimental condiation: MPOPS: 2 mg; MB: 40 ppm, 20 mL, pH 7; ionic strength of all the salts: 0.1 M).

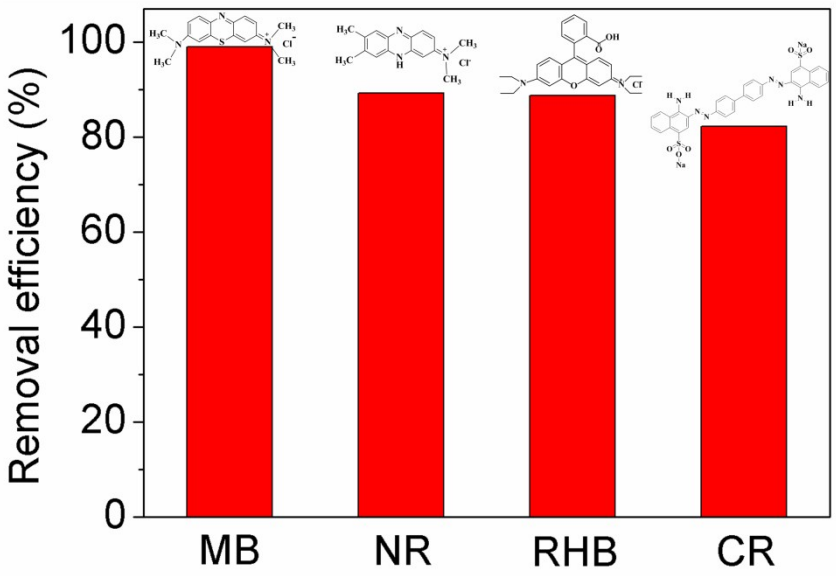

Fig. S11 Degradation efficiency of MPOPs to three organic pollutants, including Neutral Red (NR), Rhodamine B (RHB) and Congo Red (CR), at pH = 7 (20 mL, 80 ppm) for 60 min.

Table S1 The parameters of two classic kinetic models

	Pseduo-first order kinetic model			Pseduo-second order kinetic model		
	K_1/min^{-1}	R^2	q_e/mg g^{-1}	K_2/g mg^{-1} min^{-1}	R^2	q_e/mg g^{-1}
pH 2	0.036	0.9962	745	$1*10^{-4}$	0.9712	770
pH 4	0.156	0.9994	795	$3*10^{-4}$	0.9987	770
pH 6	0.182	0.9997	795	$8*10^{-4}$	0.9978	770
pH 7	0.290	0.9999	795	$3*10^{-3}$	0.9983	770
pH 10	0.427	0.9999	795	$8*10^{-3}$	0.9983	770
Fe^{2+} pH 4	0.161	0.9977	786	$3*10^{-4}$	0.9847	770
Fe^{2+} pH 7	$3*10^{-3}$	0.9847	443	$7*10^{-5}$	0.9107	476
Fe_3O_4, pH 7	$7.83*10^{-4}$	0.9999	156	$4*10^{-3}$	0.9881	163

Table S2 The exhibition of catalytic performance of different iron oxide based materials.

Catalysts/mass	Dye concentration/ volume	Time	Dye removal rate	pH	Removal capacity ($mg\ g^{-1}$)
[2]MPCMS-500/20 mg	40 ppm, 10 mL	40 min	100 %	5	20
[3]Fe_3O_4@PDA-MnO_2/ 5 mg	40 ppm, 25 mL	30 min	94 %	2-12	200
[4]Fe_3C/C/10 mg	20 ppm, 100 mL	50 min	100 %	2-12	200
	150 ppm, 100 mL	200 min	56 %		660
[5]$TA_{0.02}$- Fe_3O_4/10 mg	40 ppm, 10 mL	12.5 min	100 %	3-7	40
[6]Fe_2O_3@mesoporous silica/10 mg	50 ppm, 20 mL	420 min	90 %	-	100
[7]$Fe_{2.22}Ti_{0.78}O_4$/1.2 g	100 ppm, 400 mL	60 min	98 %	7	3.3
[8]TEA/GO/@Fe_3O_4/ 10 mg	100 ppm, 50 mL	5 min	99 %	4	500
[9]Fe^0- Fe_3O_4-RGO/ 10 mg	50 ppm, 100 mL	60 min	98 %	3	500
[10]Fe_3O_4/Fe/Fe_3C@ PCNF/40 mg	100 ppm,40 mL	30	98 %	4.5	100
MPOPs/2 mg (This work)	40 ppm, 20 mL	10	99 %	2-10	400
	300 ppm, 20 mL	60	87 %		2600

Table S3 The exhibition of Fe-leaching experiment data of different iron based materials.

	[Fe, ppm] Catalyst	[Fe, ppm] Dissolved	Iron loss %
[11]Fe-NaY	7.6	2.1	27.6
[12]Fe_2O_3/γ-Al_2O_3	20	5	20
[11]Fe-TS-1	3.8	0.6	15.7
[13]$CuFe_2O_4$	23.5	1.8	7.6
[14]Fe_3O_4@CeO_2	620	11.8	1.9
MPOPs	27.4	0.4	1.4

References

1 (a)J. L. L. Xiao, D. F. Brougham, E. K. Fox, N. Feliu, A. Bushmelev,, N. M. A. Schmidt, F. Kiessling, M. Valldor, B. Fadeel and and S. Mathur, *ACS Nano*, 2011, **5**, 6315-6324; (b)X. L. Qiu, Q. L. Li, Y. Zhou, X. Y. Jin, A. D. Qi and Y. W. Yang, *Chem. Commun.*, 2015, **51**, 4237-4240.

2 L. Zhou, Y. Shao, J. Liu, Z. Ye, H. Zhang, J. Ma, Y. Jia, W. Gao and Y. Li, *ACS Appl. Mater. Interfaces*, 2014, **6**, 7275-7285.

3 X. Pan, S. Cheng, T. Su, G. Zuo, W. Zhao, X. Qi, W. Wei and W. Dong, *Colloid Surf. B-Biointerfaces*, 2019, **181**, 226-233.

4 W. Huang, F. Wang, N. Qiu, X. Wu, C. Zang, A. Li and L. Xu, *J. Hazard. Mater.*, 2019, **378**, 120728.

5 C. Hou, Y. Wang, H. Zhu and H. Wei, *J. Taiwan Inst. Chem. Eng.*, 2016, **60**, 438-444.

6 Z. M. Cui, Z. Chen, C. Y. Cao, L. Jiang and W. G. Song, *Chem. Commun.*, 2013, **49**, 2332-2334.

7 S. Yang, H. He, D. Wu, D. Chen, X. Liang, Z. Qin, M. Fan, J. Zhu and P. Yuan, *Appl. Catal. B-Environ.*, 2009, **89**, 527-535.

8 Z. Cao, X. Wen, P. Chen, F. Yang, X. Ou, S. Wang and H. Zhong, *Colloid Surf. A-Physicochem. Eng. Asp.*, 2018, **549**, 94-104.

9 B. Yang, Z. Tian, L. Zhang, Y. Guo and S. Yan, *Journal of Water Process Engineering*, 2015, **5**, 101-111.

10 S. H. Yoo, D. Jang, H. Joh and S. Lee, *J. Mater. Chem. A*, 2017, **5**, 748-755.

11 J. L. S. Gabriel Ovejero, Fernando Martı´nez, Juan A. Melero, and and L. Gordo, *Ind. Eng. Chem. Res.*, 2001, **40**, 3921-3928.

12 M. Lu, Y. Yao, L. Gao, D. Mo, F. Lin and S. Lu, *Water Air Soil Pollut.*, 2015, **226**, 87.

13 M. A. Fontecha-Cámara, C. Moreno-Castilla, M. V. López-Ramón and M. A. Álvarez, *Appl. Catal. B-Environ.*, 2016, **196**, 207-215.

14 L. Xu and J. Wang, *Environ. Sci. Technol.*, 2012, **46**, 10145-10153.